High fidelity multi-qubit neutral atom gates

X. Jiang,[1] M. Otten,[2] and M. Saffman[1,3]

[1] *Department of Physics, University of Wisconsin-Madison, Madison, Wisconsin 53706*
[2] *HRL Laboratories, LLC, 3011 Malibu Canyon Road, Malibu, CA 90265*
[3] *ColdQuanta, Inc., 111 N. Fairchild St., Madison, Wisconsin 53703*

(Dated: August 5, 2022)

We analyze two complementary protocols for multi-qubit neutral atom gates that achieves fidelity above the threshold for fault tolerance with available quantum error correcting codes and experimentally realistic parameters. One protocol uses a pair of adiabatic pulses to implement $\mathsf{C}_k\mathsf{Z}$ gates with k control qubits acting on a single target, and the other uses single Gaussian pulses to implement CZ_k gates with one control qubit acting on k targets. We show that fidelity $\mathcal{F} > 0.99$ can be achieved for both protocols with gate times < 0.5 μs for $k \leq 4$. The residual errors include leakage out of the computational basis. A novel repumping scheme is introduced that converts leakage errors into depolarizing errors.

I. INTRODUCTION

Many quantum algorithms, as well as codes for quantum error correction, benefit from the availability of multi-qubit gates. Although such gates can always be expressed as a sequence of one- and two-qubit operations[1], the decomposition may not be as efficient as a hardware native implementation. Neutral atom qubits provide a natural setting for efficient implementation of multi-qubit gates using the strong and long range nature of the Rydberg blockade mechanism[2, 3], which enabled several early proposals for multi-qubit interactions[4, 5]. More recently a large number of proposals for multi-qubit Rydberg gates have emerged [6–19], as well as an experimental demonstration of a 3-qubit Toffoli gate[20].

In this paper we propose and analyze a high fidelity approach for implementing $\mathsf{C}_k\mathsf{Z}$ gates and CZ_k gates. A $\mathsf{C}_k\mathsf{Z}$ gate performs a Z rotation on the target qubit when all $k+1$ qubits are in state $|1\rangle$, and otherwise does not change the state of the target. Since the phase of a multi-qubit state is a shared property, $\mathsf{C}_k\mathsf{Z}$ is symmetric with respect to relabeling of the qubits, a property that is also shared with the standard two-qubit $\mathsf{C}_1\mathsf{Z} \equiv \mathsf{CZ}$ gate. The $\mathsf{C}_k\mathsf{Z}$ gate can be converted into a $\mathsf{C}_k\mathsf{X}$ gate with single qubit rotations using $\mathsf{C}_k\mathsf{X} = (\mathsf{I}^{\otimes^k} \otimes \mathsf{H})\mathsf{C}_k\mathsf{Z}(\mathsf{I}^{\otimes^k} \otimes \mathsf{H})$. The $\mathsf{C}_k\mathsf{X}$ gate appears in error correction circuits and is useful for implementation of Grover's algorithm[21].

The CZ_k gate acting on a $1+k$ qubit state imparts a phase shift according to $\mathsf{CZ}_k|\psi\rangle = e^{\imath\phi}|\psi\rangle$ with $\phi = n\pi$ where $n = 0$ if the control qubit is in state $|0\rangle$ and n is equal to the number of target qubits in state $|1\rangle$ otherwise. This gate can be converted into CX_k using $\mathsf{CX}_k = (\mathsf{I}\otimes\mathsf{H}^{\otimes^k})\mathsf{CZ}_k(\mathsf{I}\otimes\mathsf{H}^{\otimes^k})$. The CX_k gate with $k = 4$ is a basic operation for measuring X stabilizers in a surface code plaquette[22].

In Sec. II we show that both of these multi-qubit operations can be implemented very efficiently, and with high fidelity, for $k \leq 4$ using adiabatic laser pulses that are applied simultaneously to all of the qubits. Decomposition of $\mathsf{C}_k\mathsf{X}$ into elementary gates has a CX cost $\geq 2k+2$ [23] so the implementation presented here is potentially much more efficient. While CZ_k can be decomposed into sequential application of k CZ gates the multi-qubit gate implementation has the potential for an operational speedup of order k. Master equation simulations of gate performance based on physically realistic models, including leakage to spectator atomic states are presented. Gate performance depends on the variation of the coupling strength between different atom pairs. Atomic geometries and Rydberg levels are identified that provide desired interaction maps, and departures from the ideal case are studied numerically.

Gate errors are dominated by a combination of coherent control errors and leakage out of the computational subspace. The balance between coherent and leakage errors can be controlled to a certain extent by appropriate choice of gate parameters. These leakage errors can be converted into depolarization errors using a novel repumping scheme presented in Sec. IV.

For $\mathsf{C}_k\mathsf{Z}$ gates the gate fidelity is optimal when all $k+1$ qubits are coupled to each other with equal strength interactions, while for CZ_k gates the fidelity is optimal when the coupling between the k target qubits is exactly zero. In a planar qubit array these conditions are not trivial to achieve for $k > 2$. Plaquette designs and calculations of the achievable uniformity of the Rydberg interaction, as well as the impact on gate fidelity are presented in Sec. V. The results are summarized in Sec. VI.

II. $\mathsf{C}_k\mathsf{Z}$ GATE PROTOCOL

A $\mathsf{C}_k\mathsf{Z}$ gate involves $k+1$ qubits with a controlled Z operation performed on the target provided all $k+1$ qubits are in state $|1\rangle$. This can be expressed as

$$\mathsf{C}_k\mathsf{Z} = \mathsf{I} - 2\mathsf{P}_{|1\rangle^{\otimes(k+1)}} \tag{1}$$

where I is the identity operator and $\mathsf{P}_{|1\rangle^{\otimes(k+1)}}$ is the projector onto the state $|1\rangle^{\otimes(k+1)}$.

The $\mathsf{C}_k\mathsf{Z}$ gate can be realized in a system with symmetric interactions, where all the $k+1$ atoms are within a

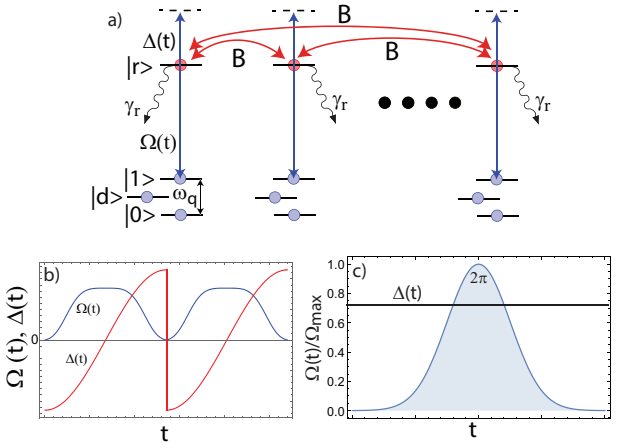

Figure 1. Multi-qubit gate protocols. a) Each atom is described with a 4-level structure: computational basis $|0\rangle$, $|1\rangle$, Rydberg state $|r\rangle$, and leakage state $|d\rangle$. In the fully symmetric case each pair of atoms has equal Rydberg coupling B. b) ARP pulses applied to each atom for the $\mathsf{C}_k\mathsf{Z}$ gate. c) Single Gaussian pulse at fixed detunig applied to each atom for the CZ_k gate.

blockade radius of each other. To implement the gate, 2π Rydberg pulses are applied to each atom, and the system is coupled to a collective, singly excited Rydberg state. After the pulse the collective state gains a π phase shift, except when the initial state of the system is $|00...0\rangle$, assuming that the Rydberg pulse couples state $|0\rangle$ to Rydberg state $|r\rangle$. Therefore the logical transformation matrix of the system is diag$[-1,-1,-1,...,1]$, which is equivalent to a $\mathsf{C}_k\mathsf{Z}$ gate, up to an irrelevant global phase. Although the Rydberg blockade mechanism is an essential ingredient that enables this multi-qubit gate it also leads to a Rabi frequency and pulse area that scales as $\sqrt{n}$ where n is the number of Rydberg coupled atoms. Since n is unknown the pulse area is not well defined, which leads to large gate errors if constant amplitude pulses are used. This problem can be circumvented by using adiabatic pulses which have a constant pulse area despite the underlying variation in Rabi frequency. This idea was introduced in[24] in the context of gate design for multi-atom ensemble qubits.

We consider two types of adiabatic pulses shown in Fig. 1: the double ARP pulse analyzed in [25] with Bell-state fidelity $\mathcal{F} > 0.997$ and the single Gaussian pulses analyzed in [26] with fidelity $\mathcal{F} > 0.996$. The ARP pulses consist of two identical π pulses with time-dependent Rabi drive $\Omega(t)$ and detuning $\Delta(t)$

$$\Omega(t) = \Omega_0 \frac{e^{-(t-t_0)^4/\tau^4} - a}{1-a} \tag{2a}$$

$$\Delta(t) = -\Delta_0 \cos\left(\frac{2\pi}{T}t\right), \tag{2b}$$

with t_0 the center of each pulse and T/2 the length of each pulse so the gate duration is T. The parameter a is chosen so that $\Omega = 0$ at the beginning and end of each pulse. The pulse slope parameter was set to be $\tau = 0.175T$. **ms** was this value of τ always used ?

The single Gaussian pulse has a constant detuning $\Delta(t) = \Delta$ and a time-dependent Rabi Drive

$$\Omega(t) = \Omega_0 e^{-t^2/\delta t^2}. \tag{3}$$

The parameter δt was varied to optimize the gate fidelity as discussed below.

Multi-qubit $\mathsf{C}_k\mathsf{Z}$ and CZ_k gates act in a Hilbert space of dimension $d = 2^{k+1}$. The process fidelity can be evaluated by random sampling of the gate action on input states in a d dimensional space. It is sufficient to sample a subset of $2d$ states in mutually unbiased bases[27]. We will instead use the method introduced in [28], which shows that the average fidelity based on a set of $d+1$ input states provides a good estimate of gate fidelity. This set of states consists of $d = 2^{k+1}$ basis states $|\phi_j\rangle, j = 1, ..., 2^k$ as well as a superposition state $|\phi_{\text{ave}}\rangle = (1/\sqrt{d})\sum_{j=1}^{d}|\phi_j\rangle$. This estimate is also sufficient to quantify the nonunitarity of the gate. **ms** do we use this last feature? **ms** how were leakage errors dealt with when calculating fidelity

The Rydberg pulses used to implement $\mathsf{C}_k\mathsf{Z}$ and CZ_k gates as described below result in unitary transformations that differ from the desired outcome up to phases that can be corrected with single qubit R_Z rotations. These rotations are parameterized in terms of phases $[\chi_1, \chi_2, ..., \chi_N]$. Gate optimization is performed by varying pulse parameters and for each set of parameters also varying the χ phases to optimize the fidelity.

In the following we will show that with the ARP pulses $\mathsf{C}_k\mathsf{Z}$ fidelity $\mathcal{F} > 0.991$ can be achieved for $k = 2, 3$ and 4 with equal Rydberg coupling strengths for each pair of qubits. We will also show the protocol's robustness against unequal coupling strengths. .

A. Numerical results for symmetric interactions

In this section we start with the simplest case of equal Rydberg coupling strength between all pairs of atoms. The fidelities of the $N = k+1$ qubit gate $\mathsf{C}_k\mathsf{Z}$ for $k = 1, 2, 3, 4$ are presented in Table II A for an interaction strength of $\mathsf{B}/2\pi = 200$ MHz and in Fig.2 for $\mathsf{B}/2\pi$ from 200-600 MHz. Optimized values of the gate parameters that maximize the fidelity were found using the procedure described in Appendix A. The numerical results demonstrate that the protocol for implementing a multi-qubit $\mathsf{C}_k\mathsf{Z}$ gate with symmetric ARP pulses gives fidelities $\mathcal{F} > 0.998$. Interestingly $\mathcal{F}$ increases as k gets larger. **ms** It would be useful to add the leakage population to the table.

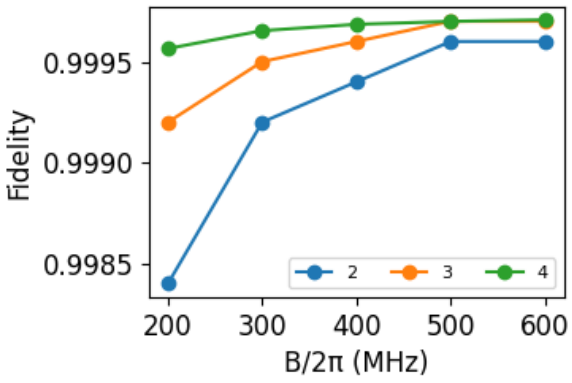

Figure 2. Numerical results for $\mathsf{C}_k\mathsf{Z}$ gate fidelities with different control qubit number k and coupling strength B. The gate is implemented with ARP pulses. $\Omega_0/2\pi = 17$ MHz, Rydberg lifetime $\tau = 540\mu s$. $T_{initial} = 0.54\mu s$, $\Delta_{initial}/2\pi = 23$ MHz.

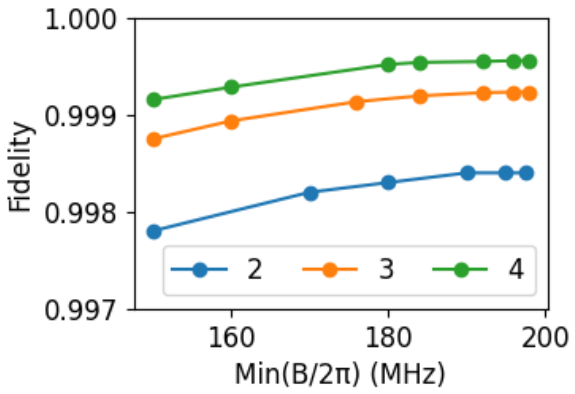

Figure 3. $\mathsf{C}_k\mathsf{Z}$ fidelity for different values of $\mathsf{B}_{\min} = \mathsf{B}_0 - \Delta\mathsf{B}$ values. Parameters are the same as in Fig. 2 with $\mathsf{B}_0/2\pi = 200$ MHz.

Table I. Fidelity of $\mathsf{C}_k\mathsf{Z}$ gates with ARP pulses for $k = 2, 3, 4$ with $\mathsf{B}/2\pi = 200$ MHz, $\Omega_0/2\pi = 17$ MHz, Rydberg lifetime $\tau = 540\mu s$. $T_{\text{initial}} = 0.54$ μs, $\Delta_{\text{initial}}/2\pi = 23$ MHz.

k	Fidelity	$\Delta_0/(2\pi)$ (MHz)	T (μs)
2	0.9984	25.36	0.399
3	0.9992	27.12	0.431
4	0.9995	28.66	0.427

B. Numerical results for asymmetric interactions

In a real implementation the interaction strengths between atom pairs may not be all equal due to geometrical constraints as well as Rydberg state dependent anisotropy of the interaction[29]. Plaquette geometries and choices of Rydberg states that give close to equal couplings are presented in Sec. V. Here we simulate the gate performance in the presence of unequal couplings to clarify the robustness of the protocol.

We start with a 3-atom case ($k = 2$) where there are 3 inter-atomic couplings and assume the coupling strengths are $\mathsf{B}_0 - \Delta\mathsf{B}$, B_0, $\mathsf{B}_0 + \Delta\mathsf{B}$. For the 4-atom case ($k = 3$), there are six inter-atomic couplings, which we assume to be $\mathsf{B}_0 - \Delta\mathsf{B}$, $\mathsf{B}_0 - 0.6\Delta\mathsf{B}$, $\mathsf{B}_0 - 0.2\Delta\mathsf{B}$, $\mathsf{B}_0 + 0,2\Delta\mathsf{B}$, $\mathsf{B}_0 + 0.6\Delta\mathsf{B}$, $\mathsf{B}_0 + \Delta\mathsf{B}$. Similarly for the 5-atom case ($k = 4$), there are 10 inter-atomic couplings that are taken to be equally spaced between $\mathsf{B}_0 - \Delta\mathsf{B}$ and $\mathsf{B}_0 + \Delta\mathsf{B}$.

Results for a range of $\Delta\mathsf{B}$ values are shown in Fig. 3. Allowing for $\Delta\mathsf{B}/\mathsf{B}_0$ up to 0.25 the reduction in fidelity is less than 0.001 for $k = 2, 3, 4$. We infer that the gate is very robust with respect to variation in the pair wise coupling strengths. We note that it is important that the coupling strengths are static, since the compensation phases needed for optimal fidelity are dependent on the values of the couplings.

III. CZ_k GATE PROTOCOL

The CZ_k gate can be expressed as ms ok ?

$$\mathsf{CZ}_k = \prod_{j=2}^{k+1} \mathsf{P}_{|1\rangle_{1j}\langle 1|} \otimes \mathsf{Z}_\mathsf{j}. \tag{4}$$

RJ: This does not look right to me since it seems to give zero when acting on the all zeros state. I'd suggest

$$\mathsf{CZ}_k = \mathsf{P}_{|0\rangle_1} \prod_{j=2}^{k+1} I_j + \mathsf{P}_{|1\rangle_1} \prod_{j=2}^{k+1} Z_j. \tag{5}$$

If the control qubit is in state $|0\rangle$ there is no operation and if both the control qubit and target qubit j are in state $|1\rangle$ a sign flip is applied to the target qubit. This seems a little confusing. I'd say based on the description in the introduction you want something like: If the control qubit is in state $|0\rangle$ there is no operation and if the control qubit is in state $|1\rangle$ and an odd number of the target qubits in state $|1\rangle$ a sign flip is applied to the state.

To achieve a CZ_k gate, a special asymmetric configuration of the inter-atomic couplings is desirable. The coupling between the control qubit and target qubits needs to be symmetric or close to symmetric, and there should be zero coupling between target qubits. If the control-target coupling is strong and the target-target coupling is zero, or sufficiently weaker, then a pulse sequence can be designed that implements a CZ_k gate. Implementations that provide asymmetric interactions can be realized in Rydberg systems where there is a great deal of flexibility in choice of atomic levels and interaction geometry[9, 30–32].

The CZ_k operation can be implemented efficiently in Rydberg blockaded qubit arrays. To implement the CZ_k gate, we generalize the 2-qubit CZ gate with symmetric pulses[]. Our simulation results show a high fidelity CZ_k gate could be achieved with the symmetric single Gaussian pulse with $\mathcal{F} > 0.99$. ♠ mention results here

Table II. Fidelity of CZ_k gate with single Gaussian pulse for $k = 2, 3, 4$ with $\mathsf{B}/2\pi = 10.75$ MHz, $\Omega_0/2\pi = 17$ MHz, Rydberg lifetime $\tau = 540\mu s$. $\delta t_{initial} = 0.2\mu s$, $\Delta_{initial}/2\pi = 23$ MHz

k	Fidelity	$\Delta_0/(2\pi)$ (MHz)	T (μs)
2	0.9988	25.36	0.399
3	0.9928	27.12	0.431
4	0.9974	28.66	0.427

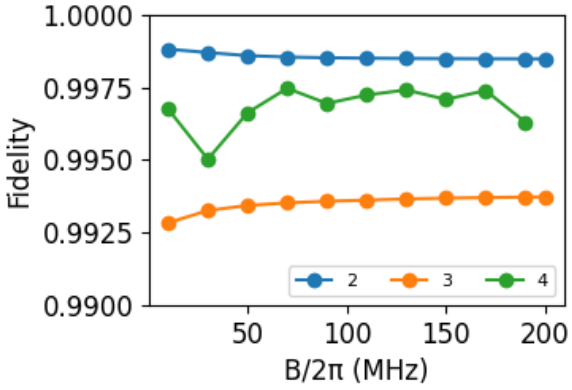

Figure 4. Numerical results for CZ_k gate with different target qubit number k and coupling strength B. $\Omega_0/2\pi = 17$ MHz, Rydberg lifetime $\tau = 540\mu s$. $\delta t_{initial} = 0.2\mu s$, $\Delta_{initial}/2\pi = 23$ MHz.

A. Numerical results with zero target-target couplings

In this section we start with the simplest case where the Rydberg coupling strength is exactly zero between all pairs of target qubits. The results are shown in Fig.4 and Table III A. ♠ The results are...

B. Numerical results with finite target-target couplings

In this section we study the nonideal case where the coupling between two target qubits is not negligible. For simplicity we assume that all target-target coupling strengths are the same, and equal to a fraction ϵ of the control-target interaction strength. We then vary ϵ and repeat the optimization in the above section for each value. From the results in Fig. 5 we see that the CZ_k fidelity remains above 0.99 for $k = 2, 3, 4$ and $\epsilon < 0.25$.

IV. QUBIT PUMPING

Rydberg gate errors arise primarily from two effects. The first is coherent rotation errors due to variations in the amplitude or frequency of the laser pulses or due to variations in the atom separation which changes the Rydberg interaction strength. The second type of error arises

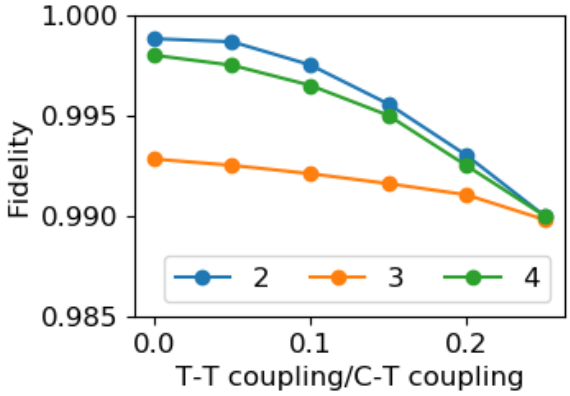

Figure 5. Fidelities at different target-target(T-T) coupling values as a percentage of control-target(C-T) coupling for k=2,3 and 4 with the single Gaussain pulse. $B_0/2\pi = 10.5$ MHz.

from spontaneous emission that scales as the ratio t_r/τ where t_r is the effective time that population is in the Rydberg state during the gate, and τ is the Rydberg lifetime. Spontaneous emission also occurs due to scattering from intermediate states that facilitate two-photon Rydberg excitation. The intermediate state scattering can be suppressed far below the scattering from the Rydberg state by using a large one-photon detuning from the intermediate state[34]. Therefore only the Rydberg scattering is included in this analysis.

Spontaneous emission events can be divided into two types. There is redistribution of population between the qubit states leading to depolarization errors as well as population of Zeeman substates that are outside the computational basis leading to leakage errors. As has been emphasized recently[35], detectable leakage errors lead to higher code thresholds than depolarization errors, provided the leakage sites are subsequently reinitialized in the computational basis. Leakage due to physical loss of an atom requires atom replacement. Leakage into a Zeeman state outside the computational basis, can be repaired using the pumping procedure shown in Fig. 6. In the ideal limit this procedure does not change a valid qubit state, but repumps states outside the computational basis into a superposition of qubit states thereby converting leakage errors into depolarization errors.

The basic idea is illustrated in Fig. 6. A pair of π polarized optical fields couple $6s_{1/2}, f = 3$ to $6p_{1/2}, f' = 3$ and $6s_{1/2}, f = 4$ to $6p_{1/2}, f' = 4$. Due to selection rules the matrix element is zero for π transitions between states with $f = f'$ and $m = 0$. Therefore any population in a valid qubit state will be largely unaffected while population in states with $m \neq 0$ will be excited to the $6p_{1/2}$ level and decay back to the ground level. The Zeeman state can change by $-1, 0, 1$ in the decay so population accumulates in a qubit state. The dynamics can be analyzed by solving the Lindblad equation or, to a good approximation, using rate equations.

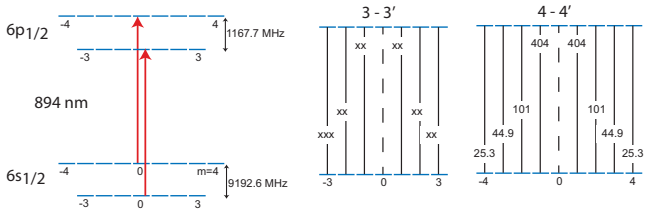

Figure 6. (color online) Atomic structure for qubit pumping with Cs atoms. The transitions are labeled with the saturation intensity in W/m^2. The saturation intensity of the transition $|fm\rangle \to |f'm\rangle$ is $I_{fm,f'm} = \epsilon_0 c\hbar^2\gamma^2/4d^2_{fm,f'm}$ with $d_{fm,f'm}$ the dipole matrix element, and γ the natural linewidth of the $6p_{1/2}$ level.♠ need to add values for 3 to 3'

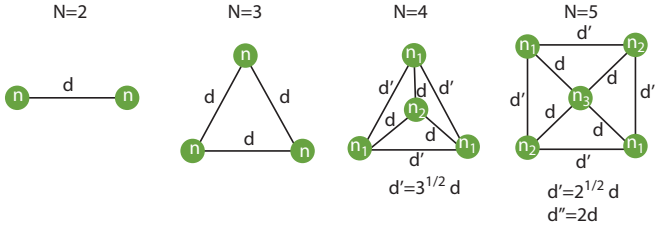

Figure 7. Geometrical arrangements and choice of Rydberg states for $N = 2, 3, 4, 5$. Using Rydberg ns states with isotropic interactions equal couplings can be achieved for $N = 2, 3, 4$. For $N = 5$ close to equal couplings are possible as discussed in the text.

Leakage events during a Rydberg gate can result in population transferring to any $m \neq 0$ state since the decay process may involve multiple transitions. For highly excited Rydberg states in a room temperature environment roughly half of the decay is to the ground state or first optically excited states and half is driven by blackbody radiation to nearby Rydberg levels, that then decay, or transfer further to other levels. We therefore expect that the distribution among Zeeman states will be peaked close to $m = 0$ and substantially smaller for larger $|m|$. For simplicity we will use a conservative model that assumes equal distribution among Zeeman states. This implies that with probability 1/16 a spontaneous emission leads to a Z error, probability 1/16 a depolarization error, and probability 7/8 a leakage error. The pumping procedure converts leakage errors into depolarization errors so the error model becomes Z errors with probability 1/16 and depolarization errors with probability 15/16.

♠ mark add rate equation results

V. PLAQUETTE GEOMETRIES FOR UNIFORM RYDBERG INTERACTIONS

The multi-qubit protocols described in the following sections operate with the highest fidelity when all atom pairs have an equal strength Rydberg coupling. The interaction strength between atomic Rydberg states depends on the principal quantum number, the interatomic separation, and the geometrical orientation[29]. For alkali atom s orbitals the interaction is very close to isotropic and depends monotonically on the separation R as $1/R^3$ at short range and $1/R^6$ at long range.

Figure 7 shows qubit layouts in 2D that can be used to achieve close to equal coupling strengths, and can be used to tile the plane, thereby supporting a scalable qubit register.

For implementation of multi-qubit gates the simplest situation is equal coupling between all atoms. This is automatically the case for $N = 2$ atoms and trivially possible for $N = 3$ using a planar triangular arrangement. For $N > 3$ it is not possible to find a planar geometry that gives equal distances between all atom pairs.

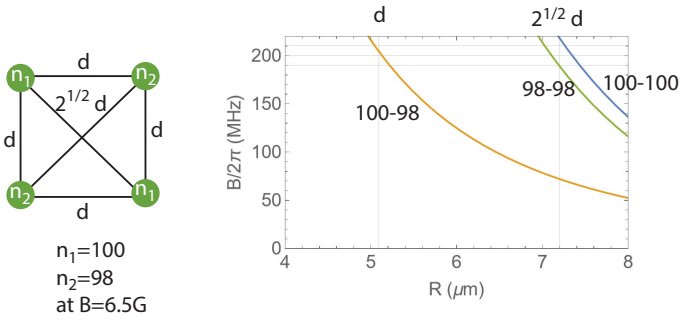

Figure 8. Choice of Rydberg states for the 4-qubit case. Using Cs $98s$ and $100s$ in a field of $B_z = 6.5$ G all coupling strengths are equalized to within about 5%.

Symmetric interactions can be achieved by coupling to several different Rydberg states as shown in Fig. 7. For $N = 4$ atoms we excite states $n_1 s$ and $n_2 s$ where n_1, n_2 are the principal quantum numbers. The interaction strengths are $V_1 = V_{n_1,n_1}(\sqrt{2}d)$, $V_2 = V_{n_2,n_2}(\sqrt{2}d)$, and $V_3 = V_{n_1,n_2}(d)$. The interaction between two atoms in the same Rydberg state has a strong dependence on n but if $n_2 = n_1 \pm 1$ and n_1 is large the small fractional difference between V_{n_1,n_1} and V_{n_2,n_2} scales as $1/n_1$. On the other hand the interaction between different Rydberg states decreases rapidly with $|n_2 - n_1|$. The interaction strength also depends on the angle θ between the interatomic axis the quantization axis. We will assume the $m_a = m_b = 1/2$ Rydberg Zeeman states (a, b denote the atoms) are excited with the quantization axis perpendicular to the plane containing the atoms, thus $\theta = \pi/2$. As shown in [36] the interaction at $\theta = \pi/2$ can be either enhanced or suppressed relative to $\theta = 0$ depending on the values of the energy defects and C_3 coefficients for the Förster eigenstates. This additional freedom will allow us to pick states that provide better matching of the interaction strengths. Details of the calculations are given in Appendix **??**.

Here is a first attempt at finding parameters for the 4-qubit case.

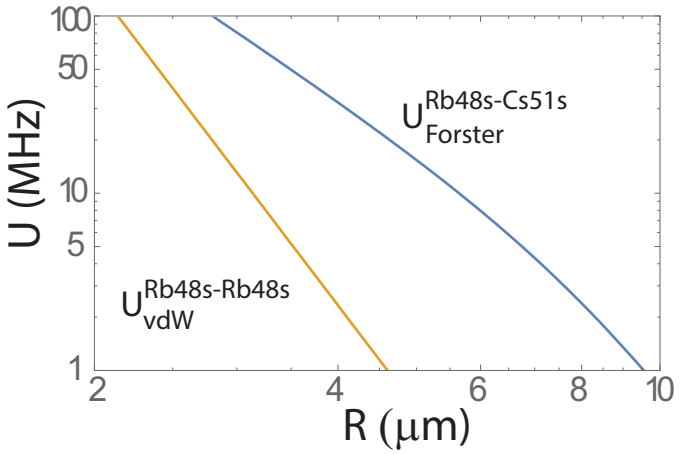

Figure 9. Rb-Cs coupling strengths

VI. DISCUSSION

Appendix A: Optimization Method

In the numerical simulations, we use the following method for optimizing gate fidelities. First, we choose a set of fixed parameters for the simulation. For both CZ_k and $\mathsf{C}_k\mathsf{Z}$ gates these parameters include Rabi frequency Ω_0, ancilla-data qubit coupling strength B, Rydberg lifetime τ and the value of k.

Second, we choose a set of initial pulse parameters, which are δ_t and Δ for the CZ_k gates and T and Δ for the $\mathsf{C}_k\mathsf{Z}$ gates, and calculate the average fidelity of the multi-qubit gates introduced in [28]. We then optimize by changing the correction phases $[\chi_1, \chi_2, ..., \chi_{k+1}]$, which corresponds to the single-qubit rotation phases that can be done to each of the qubits to maximize the gate fidelity.

Finally, after optimizing the gate fidelity over the individual phases for the initial parameters, we vary the initial parameters, optimize over the phases for each case and find the optimal parameters for gate fidelity.

ms need description of search method. gradient descent? Nelder-Mead?

Appendix B: Parameters for CZ_k gate with single Gaussian pulses

The CZ_k gate parameters for each point on Fig.4 and Fig.5 are shown in Table.B-B.

Appendix C: Parameters for $\mathsf{C}_k\mathsf{Z}$ gate with ARP pulses

The $\mathsf{C}_k\mathsf{Z}$ gate parameters for each point on Fig.2 and Fig.3 are shown in Table.C-C.

Appendix D: Sensitivity of CZ_k and $\mathsf{C}_k\mathsf{Z}$ gates to phase variations

We vary the single-qubit rotation phase of the control qubit and the first target qubit to check the sensitivity of CZ_k and $\mathsf{C}_k\mathsf{Z}$ gates to single qubit phase variations. The results are shown in Fig.10 and Fig.11.

ACKNOWLEDGMENTS

We acknowledge helpful discussion with Robert Joynt. This material is based upon work supported by the U.S. Department of Energy Office of Science National Quantum Information Science Research Centers and support from NSF Award 2016136 for the QLCI center Hybrid Quantum Architectures and Networks.

[1] A. Barenco, C. H. Bennett, R. Cleve, D. P. DiVincenzo, N. Margolus, P. Shor, T. Sleator, J. A. Smolin, and H. Weinfurter, "Elementary gates for quantum computation," Phys. Rev. A **52**, 3457–3467 (1995).

[2] M. D. Lukin, M. Fleischhauer, R. Cote, L. M. Duan, D. Jaksch, J. I. Cirac, and P. Zoller, "Dipole blockade and quantum information processing in mesoscopic atomic ensembles," Phys. Rev. Lett. **87**, 037901 (2001).

[3] M. Saffman, T. G. Walker, and K. Mølmer, "Quantum information with Rydberg atoms," Rev. Mod. Phys. **82**, 2313–2363 (2010).

[4] E. Brion, A. S. Mouritzen, and K. Mølmer, "Conditional dynamics induced by new configurations for Rydberg dipole-dipole interactions," Phys. Rev. A **76**, 022334 (2007).

[5] L. Isenhower, M. Saffman, and K. Mølmer, "Multibit C_kNOT quantum gates via Rydberg blockade," Quant. Inf. Proc. **10**, 755 (2011).

[6] S.L. Su, H.Z. Shen, L. Erjun, and Z. Shou, "One-step construction of the multiple-qubit Rydberg controlled-

Table III. Parameters for CZ_k gate with single Gaussian pulse for $k = 2$, $\Omega_0/2\pi = 17$ MHz, $\delta t_{initial} = 0.2\mu s$, $\Delta_{initial}/\Omega = 0.5$

$B/(2\pi)$ (MHz)	Fidelity	Δ/Ω	δt (μs)	ϕ_1	ϕ_2	ϕ_3
10.75	0.9988	0.2383	0.3139	1.1188	-1.8854	-1.8854
20	0.9988	0.4334	0.4067	1.3494	-1.6466	-1.6466
30	0.9987	0.5032	0.4097	-0.0577	-3.0456	-3.0456
40	0.9986	0.5475	0.4113	-0.8702	2.4288	2.4289
50	0.9986	0.5785	0.4124	-1.4052	1.8966	1.8966
60	0.9986	0.6016	0.4131	-1.7885	1.5151	1.5152
70	0.9985	0.6196	0.4137	-2.0763	1.2283	1.2284
80	0.9985	0.6341	0.4141	-2.3013	1.0041	1.0041
90	0.9985	0.6459	0.4144	-2.4851	0.8207	0.8207
100	0.9985	0.6558	0.4147	3.6503	0.6738	0.6739
110	0.9985	0.6643	0.4149	3.5249	0.5486	0.5485
120	0.9985	0.6716	0.4151	3.4177	0.4415	0.4416
130	0.9985	0.6780	0.4153	3.3266	0.3506	0.3508
140	0.9985	0.6835	0.4155	3.2464	0.2706	0.2706
150	0.9985	0.6884	0.4156	3.1754	0.1996	0.1996
160	0.9985	0.6927	0.4156	3.1130	0.1374	0.1375
170	0.9985	0.6966	0.4158	3.0579	0.0828	0.0829
180	0.9985	0.7002	0.4158	3.0067	0.0312	0.0313
190	0.9985	0.7034	0.4159	2.9629	-0.0121	-0.0123
200	0.9985	0.7064	0.4160	2.9220	-0.0529	-0.0527

Table IV. Parameters for CZ_k gate with single Gaussian pulse for $k = 3$, $\Omega_0/2\pi = 17$ MHz, $\delta t_{initial} = 0.2\mu s$, $\Delta_{initial}/\Omega = 0.5$

$B/(2\pi)$ (MHz)	Fidelity	Δ/Ω	δt (μs)	ϕ_1	ϕ_2	ϕ_3	ϕ_4
10	0.9928	0.4979	0.1680	0.1090	-1.6459	-1.6459	-1.6458
20	0.9931	0.5098	0.1425	-1.3888	3.3518	3.3518	3.3519
30	0.9932	0.5315	0.1395	-1.8388	3.0485	3.0483	3.0485
40	0.9934	0.5475	0.1370	-2.1406	2.8189	2.8193	2.8191
50	0.9934	0.5594	0.1349	-2.3549	2.6464	2.6466	2.6467
60	0.9935	0.5682	0.1331	-2.5160	2.5125	2.5125	2.5126
70	0.9935	0.5750	0.1316	-2.6408	2.4063	2.4061	2.4064
80	0.9935	0.5802	0.1303	-2.7438	2.3164	2.3163	2.3162
90	0.9936	0.5841	0.1290	-2.8296	2.2401	2.2399	2.2401
100	0.9936	0.5874	0.1278	-2.9054	2.1703	2.1702	2.1701
110	0.9936	0.5897	0.1267	-2.9715	2.1086	2.1087	2.1087
120	0.9936	0.5696	0.1137	2.9517	1.6890	1.6889	1.6889
130	0.9937	0.5709	0.1136	2.9255	1.6744	1.6744	1.6743
140	0.9937	0.5721	0.1135	2.9027	1.6615	1.6619	1.6617
150	0.9937	0.5734	0.1133	2.8815	1.6484	1.6485	1.6483
160	0.9937	0.5744	0.1133	2.8638	1.6382	1.6381	1.6382
170	0.9937	0.5753	0.1132	2.8472	1.6277	1.6280	1.6278
180	0.9937	0.5762	0.1130	2.8318	1.6181	1.6179	1.6181
190	0.9937	0.5770	0.1130	2.8185	1.6099	1.6098	1.6097
200	0.9937	0.5777	0.1129	2.8068	1.6029	1.6028	1.6028

Table V. Parameters for CZ_k gate with single Gaussian pulse for $k = 4$, $\Omega_0/2\pi = 17$ MHz, $\delta t_{initial} = 0.2\mu s$, $\Delta_{initial}/\Omega = 0.5$

$B/(2\pi)$ (MHz)	Fidelity	Δ/Ω	δt (μs)	ϕ_1	ϕ_2	ϕ_3	ϕ_4	ϕ_5
10	0.9967	0.5045	0.2222	2.0155	0.5987	0.5987	0.5987	0.5985
30	0.9950	0.5045	0.2222	0.5926	0.3988	0.3984	0.3987	0.3986
50	0.9966	0.5654	0.1654	-1.7351	-2.5526	-2.5523	-2.5522	-2.5521
70	0.9975	0.6000	0.1101	2.8183	1.3092	1.3090	1.3092	1.3088
90	0.9969	0.5358	0.1214	3.0567	2.0636	2.0635	2.0633	2.0631
110	0.9942	0.5899	0.2278	-0.6421	-0.3472	-0.3471	-0.3469	-0.3472
150	0.9971	0.5585	0.1184	2.7948	1.8082	1.8080	1.8079	1.8083

PHASE gate," Phys. Rev. A **98**, 032306 (2018).

[7] X.-F. Shi, "Deutsch, Toffoli, and CNOT gates via Rydberg blockade of neutral atoms," Phys. Rev. Applied **9**, 051001 (2018).

[8] I. I. Beterov, I. N. Ashkarin, E. A. Yakshina, D. B. Tretyakov, V. M. Entin, I. I. Ryabtsev, P. Cheinet, P. Pil-

Table VI. Fidelities for CZ_k gate with single Gaussian pulse for $k = 3, 4, 5$ with different data-data coupling strengths at $B = 10$. B is the coupling strength between control and target qubits. d-d ratio = $B_{data-data}/B$. Gate parameters are the corresponding Δ, δt and local phase numbers for $B = 10$ in Table B, B and B

d-d ratio	Fidelity($k = 2$)	Fidelity($k = 3$)	Fidelity($k = 4$)
0	0.9988	0.9928	0.9938
0.05	0.9987	0.9925	0.9934
0.1	0.9975	0.9921	0.9926
0.15	0.9956	0.9916	0.9916
0.2	0.9930	0.9910	0.9904
0.25	0.9900	0.9904	0.9890

Table VII. Parameters for $\mathsf{C}_k\mathsf{Z}$ gate with ARP pulse for $k = 2$, $\Omega_0/2\pi = 17$ MHz, $T_{initial} = 0.54\mu s$, $\Delta_{initial} = 23$ MHz

$B/(2\pi)$ (MHz)	Fidelity	$\Delta/(2\pi)$ (MHz)	δt (μs)	ϕ_1	ϕ_2	ϕ_3
200	0.9984	23.7883	0.5095	0.4628	0.4625	0.4625
300	0.9992	23.2001	0.5185	0.3127	0.3128	0.3128
400	0.9994	23.1993	0.5212	0.2355	0.2358	0.2356
500	0.9996	23.1606	0.5226	0.1890	0.1887	0.1890
600	0.9996	23.2264	0.5235	0.1578	0.1575	0.1576

Table VIII. Parameters for $\mathsf{C}_k\mathsf{Z}$ gate with ARP pulse for $k = 3$, $\Omega_0/2\pi = 17$ MHz, $T_{initial} = 0.54\mu s$, $\Delta_{initial} = 23$ MHz

$B/(2\pi)$ (MHz)	Fidelity	$\Delta/(2\pi)$ (MHz)	δt (μs)	ϕ_1	ϕ_2	ϕ_3	ϕ_4
200	0.9992	23.9516	0.5312	0.5634	0.5634	0.5632	0.5634
300	0.9995	23.8794	0.5350	0.3769	0.3767	0.3769	0.3769
400	0.9996	23.9011	0.5365	0.2832	0.2830	0.2828	0.2830
500	0.9997	23.9184	0.5376	0.2266	0.2267	0.2268	0.2268
600	0.9997	23.9621	0.5387	0.1890	0.1892	0.1893	0.1894

Table IX. Parameters for $\mathsf{C}_k\mathsf{Z}$ gate with ARP pulse for $k = 4$, $\Omega_0/2\pi = 17$ MHz, $T_{initial} = 0.54\mu s$, $\Delta_{initial} = 23$ MHz

$B/(2\pi)$ (MHz)	Fidelity	$\Delta/(2\pi)$ (MHz)	δt (μs)	ϕ_1	ϕ_2	ϕ_3	ϕ_4	ϕ_5
200	0.9996	24.4616	0.4908	0.6134	0.6132	0.6134	0.6132	0.6131
300	0.9997	24.4448	0.5261	0.4074	0.4075	0.4074	0.4076	0.4073
400	0.9997	24.3935	0.5264	0.3051	0.3052	0.3054	0.3054	0.3053
500	0.9997	24.4084	0.5225	0.2441	0.2438	0.2439	0.2441	0.2439
600	0.9997	24.4088	0.5193	0.2035	0.2031	0.2035	0.2033	0.2032

Table X. Fidelities for $\mathsf{C}_k\mathsf{Z}$ gate with single Gaussian pulse for $k = 3, 4, 5$ with different inter-atomic coupling strengths at $B_0 = 0$. For $k = 2$, there are 3 different coupling strengths, for $k = 3$, there are 6 different coupling strengths, and for $k = 4$, there are 10 different coupling strengths. For each k number, the coupling strengths are equally spaced between $B_0 - \Delta B$ and $B_0 + \Delta B$. The Ω, Δ, T and single qubit rotation phase paramters are from the $B = 200$ cases from Table B, B and B.

$Min(B)$ for k=2	Fidelity(k=2)	$Min(B)$ for k=3	Fidelity(k=4)	$Min(B)$ for $k = 4$	Fidelity($k = 4$)
197.5	0.9984	198	0.9992	198	0.9996
195	0.9984	196	0.9992	196	0.9996
190	0.9984	192	0.9992	192	0.9995
180	0.9983	184	0.9992	184	0.9995
170	0.9982	176	0.9991	176	0.9995
150	0.9978	160	0.9989	160	0.9993

let, and M. Saffman, "Fast three-qubit Toffoli quantum gate based on three-body Förster resonances in Rydberg atoms," Phys. Rev. A **98**, 042704 (2018).

[9] M. Khazali and K. Mølmer, "Fast multiqubit gates by adiabatic evolution in interacting excited-state manifolds of Rydberg atoms and superconducting circuits," Phys. Rev. X **10**, 021054 (2020).

[10] D. Yu, Y. Gao, W. Zhang, J. Liu, and J. Qian, "Scalability and high-efficiency of an $(n+1)-$qubit Toffoli gate sphere via blockaded Rydberg atoms," arXiv:2001.04599 (2020).

[11] J. T. Young, P. Bienias, R. Belyansky, A. M. Kaufman, and A. V. Gorshkov, "Asymmetric blockade and multi-qubit gates via dipole-dipole interactions," arXiv:2006.02486 (2020).

[12] S. E. Rasmussen, K. Groenland, R. Gerritsma, K. Schoutens, and N. T. Zinner, "Single-step implementation of high-fidelity n-bit Toffoli gates," Phys. Rev. A

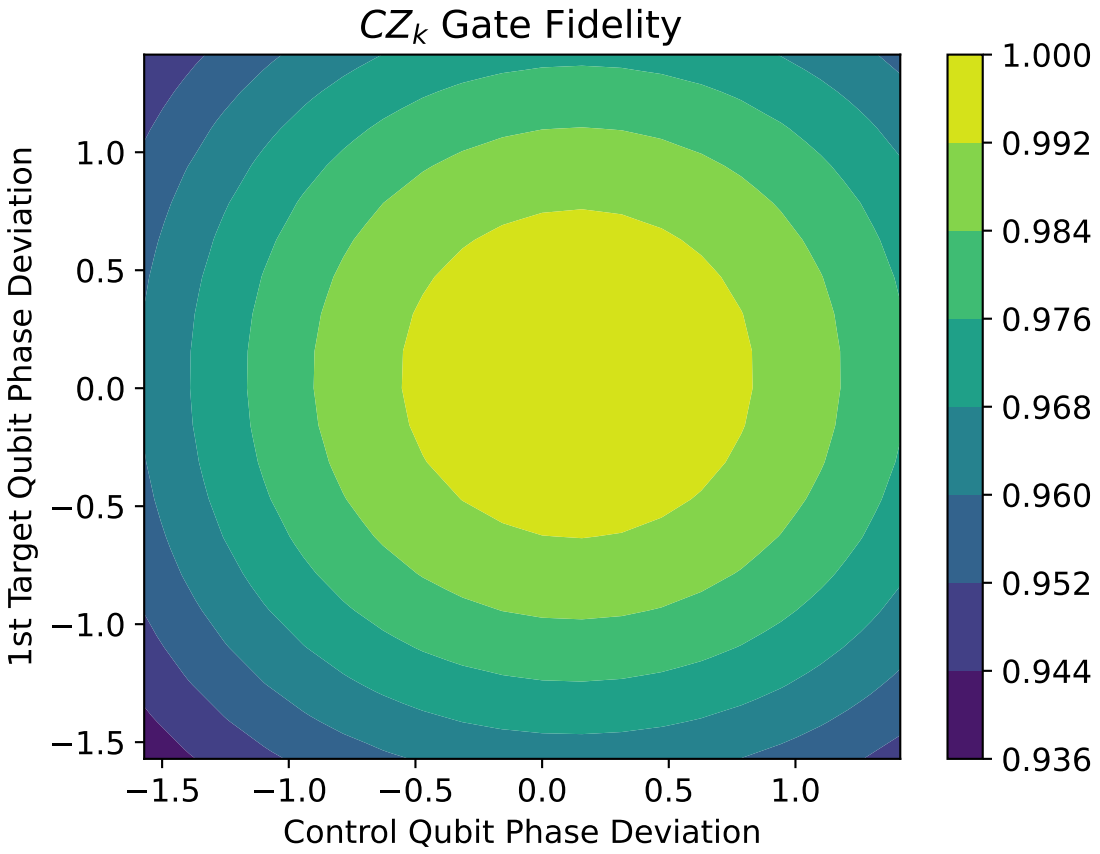

Figure 10. Fidelity of the CZ_k gate with the single Gaussian pulse with variations of the single-qubit rotation phase on the control and the first target qubit. Variation range is $[-\pi/2, \pi/2]$

101, 022308 (2020).

[13] T. H. Xing, X. Wu, and G. F. Xu, "Nonadiabatic holonomic three-qubit controlled gates realized by one-shot implementation," Phys. Rev. A **101**, 012306 (2020).

[14] H.-D. Yin, X.-X. Li, G.-C. Wang, and X.-Q. Shao, "One-step implementation of Toffoli gate for neutral atoms based on unconventional Rydberg pumping," Opt. Expr. **28**, 35576 (2020).

[15] J.-L. Wu, Y. Wang, J.-X. Han, S.-L. Su, Y. Xia, Y. Jiang, and J. Song, "Resilient quantum gates on periodically driven Rydberg atoms," Phys. Rev. A **103**, 012601 (2021).

[16] J.-L. Wu, Y. Wang, J.-X. Han, Y.-K. Feng, S.-L. Su, Y. Xia, Y. Jiang, and J. Song, "One-step implementation of Rydberg-antiblockade swap and controlled-swap gates with modified robustness," Photon. Res. **9**, 814–821 (2021).

[17] Yucheng He, Jing-Xin Liu, F.-Q. Guo, L.-L. Yan, Ronghui Luo, Erjun Liang, S.-L. Su, and M. Feng, "Multiple-qubit Rydberg quantum logic gate via dressed-states scheme," arXiv:2010.14704 (2021).

[18] M. Li, F.-Q. Guo, Z. Jin, L.-L. Yan, E.-J. Liang, and S.-L. Su, "Multiple-qubit controlled unitary quantum gate for Rydberg atoms using shortcut to adiabaticity and optimized geometric quantum operations," Phys. Rev. A **103**, 062607 (2021).

[19] G. Pelegrí, A. J. Daley, and J. D. Pritchard, "High-fidelity multiqubit Rydberg gates via two-photon adiabatic rapid passage," arXiv:2112.13025 (2022).

[20] H. Levine, A. Keesling, G. Semeghini, A. Omran, T. T. Wang, S. Ebadi, H. Bernien, M. Greiner, V. Vuletić, H. Pichler, and M. D. Lukin, "Parallel implementation of high-fidelity multiqubit gates with neutral atoms," Phys. Rev. Lett. **123**, 170503 (2019).

[21] K. Mølmer, L. Isenhower, and M. Saffman, "Efficient Grover search with Rydberg blockade," J. Phys. B: At. Mol. Opt. Phys. **44**, 184016 (2011).

[22] A. G. Fowler, M. Mariantoni, J. M. Martinis, and A. N. Cleland, "Surface codes: Towards practical large-scale quantum computation," Phys. Rev. A **86**, 032324 (2012).

[23] V. V. Shende and I. L. Markov, "On the CNOT-cost of Toffoli gates," Qu. Inf. Comput. **9**, 0461 (2009).

[24] I. I. Beterov, M. Saffman, E. A. Yakshina, V. P. Zhukov, D. B. Tretyakov, V. M. Entin, I. I. Ryabtsev, C. W. Mansell, C. MacCormick, S. Bergamini, and M. P. Fedoruk, "Quantum gates in mesoscopic atomic ensembles based on adiabatic passage and Rydberg blockade," Phys. Rev. A **88**, 010303(R) (2013).

[25] I. I. Beterov, D. B. Tretyakov, V. M. Entin, E. A. Yakshina, I. I. Ryabtsev, M. Saffman, and S. Bergamini,

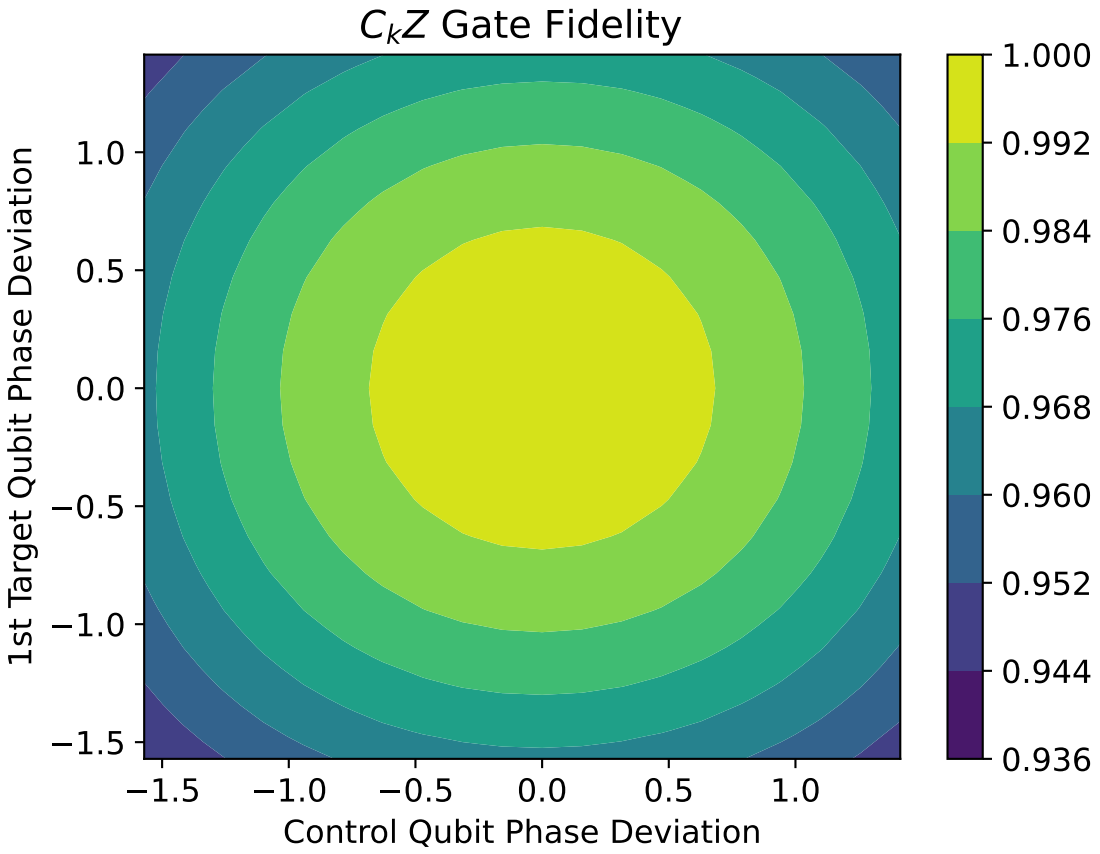

Figure 11. Fidelity of the C_kZ gate with the ARP pulse with variations of the single-qubit rotation phase on the control and the first target qubit. Variation range is $[-\pi/2, \pi/2]$

"Application of adiabatic passage in Rydberg atomic ensembles for quantum information processing," J. Phys. B: At. Mol. and Opt. Phys. **53**, 182001 (2020).

[26] F. Robicheaux, T. Graham, and M. Saffman, "Photon recoil and laser focusing limits to Rydberg gate fidelity," Phys. Rev. A **103**, 022424 (2021).

[27] H. F. Hofmann, "Complementary classical fidelities as an efficient criterion for the evaluation of experimentally realized quantum operations," Phys. Rev. Lett. **94**, 160504 (2005).

[28] D. M. Reich, G. Gualdi, and C. P. Koch, "Minimum number of input states required for quantum gate characterization," Phys. Rev. A **88**, 042309 (2013).

[29] T. G. Walker and M. Saffman, "Consequences of Zeeman degeneracy for the van der Waals blockade between Rydberg atoms," Phys. Rev. A **77**, 032723 (2008).

[30] M. Saffman and K. Mølmer, "Efficient multiparticle entanglement via asymmetric Rydberg blockade," Phys. Rev. Lett. **102**, 240502 (2009).

[31] M. Müller, I. Lesanovsky, H. Weimer, H. P. Büchler, and P. Zoller, "Mesoscopic Rydberg gate based on electromagnetically induced transparency," Phys. Rev. Lett. **102**, 170502 (2009).

[32] J. T. Young, P. Bienias, R. Belyansky, A. M. Kaufman, and A. V. Gorshkov, "Asymmetric blockade and multiqubit gates via dipole-dipole interactions," Phys. Rev. Lett. **127**, 120501 (2021).

[33] Phys. Rev. Lett..

[34] M. Saffman and T. G. Walker, "Analysis of a quantum logic device based on dipole-dipole interactions of optically trapped Rydberg atoms," Phys. Rev. A **72**, 022347 (2005).

[35] Y. Wu, W.-S. Bao, S. Cao, F. Chen, M.-C. Chen, X. Chen, T.-H. Chung, H. Deng, Y. Du, D. Fan, M. Gong, C. Guo, C. Guo, S. Guo, L. Han, L. Hong, H.-L. Huang, Yong-Heng Huo, Liping Li, Na Li, Shaowei Li, Yuan Li, Futian Liang, Chun Lin, Jin Lin, Haoran Qian, Dan Qiao, Hao Rong, Hong Su, Lihua Sun, Liangyuan Wang, Shiyu Wang, Dachao Wu, Yu Xu, Kai Yan, Weifeng Yang, Yang Yang, Yangsen Ye, Jianghan Yin, Chong Ying, Jiale Yu, Chen Zha, Cha Zhang, Haibin Zhang, Kaili Zhang, Yiming Zhang, Han Zhao, Y. Zhao, L. Zhou, Q. Zhu, C.-Y. Lu, C.-Z. Peng, X. Zhu, and J.-W. Pan, "Strong quantum computational advantage using a superconducting quantum processor," arXiv:2106.14734 (2021).

[36] I. I. Beterov and M. Saffman, "Rydberg blockade, Förster resonances, and quantum state measurements with different atomic species," Phys. Rev. A **92**, 042710 (2015).